J|A|C|S
ARTICLES
Published on Web 11/05/2002

Formation and Decay of Localized Contact Radical Ion Pairs in DNA Hairpins

Frederick D. Lewis,* Xiaoyang Liu, Scott E. Miller, Ryan T. Hayes, and Michael R. Wasielewski*

Contribution from the Department of Chemistry, Northwestern University, Evanston, Illinois 60208-3113

Received May 30, 2002

Abstract: The dynamics of charge separation and charge recombination in synthetic DNA hairpins possessing diphenylacetylene-4,4′-dicarboxamide linkers have been investigated by means of femtosecond time-resolved transient absorption spectroscopy. The lowest excited singlet state of the linker is capable of oxidizing nearest neighbor adenine as well as guanine. A large wavelength shift in the transient absorption spectrum accompanies the conversion of the singlet linker to its anion radical, facilitating the investigation of electron-transfer dynamics. The rate constants for charge separation are dependent upon the oxidation potentials of the neighboring nucleobase donors but not upon the identity of nonnearest neighbors. Thus, the charge separation processes yield a contact radical ion pair in which the positive charge is localized on the neighboring nucleobase. Rate constants for charge recombination are dependent upon the identity of the first and second nearest-neighbor nucleobases but not more remote bases. This dependence is attributed to stabilization of the contact radical ion pair by interaction with its nearest neighbor. The absence of charge migration to form a base-pair separated radical ion pair is a consequence of Coulombic attraction in the contact radical ion pair and the low effective dielectric constant ($\epsilon < 7$) experienced by the contact radical ion pair. Photoinduced charge injection to form a base-pair separated radical ion pair is necessary in order to observe charge migration.

Introduction

Photochemical oxidation or reduction of nucleobases has been widely used as a method for charge injection in DNA.[1] Our approach to the study of electron-transfer dynamics in DNA has employed femtosecond time-resolved transient absorption spectroscopy to investigate electron-transfer processes in synthetic hairpin structures in which an organic chromophore serves as the hairpin linker and electron acceptor, and a nucleobase serves as the electron donor.[2] The observation of both the initially formed lowest excited singlet state of the acceptor and its anion radical provides a method for investigation of the dynamics of charge separation, charge recombination, and charge migration processes in DNA.[3,4] We recently reported that the dynamics of charge separation and charge recombination between an excited electron acceptor and a nearest-neighbor nucleobase electron donor are dependent upon the energetics of the electron-transfer process.[5] Rate constants for charge separation increase with increasing driving force, as expected for electron-transfer processes in the Marcus normal region, whereas rate constants for charge recombination decrease with increasing driving force, as expected for electron-transfer processes in the Marcus inverted region.[6]

Theoretical studies have indicated that nucleobase ionization potentials are strongly dependent upon the identity of the neighboring nucleobase within the same strand.[7,8] Thus, the identities of both the first and second bases adjacent to the acceptor might be expected to influence the rate constants for the formation and decay of an acceptor-nucleobase contact radical ion pair. We report here an investigation of the effects of the base pair sequence on the dynamics of charge separation and charge recombination in 10 hairpin-forming bis(oligonucleotide) conjugates possessing a diphenylacetylene-4,4′dicarboxamide (DPA) linker which serves as an electron acceptor (A) and different base-paired stems (Chart 1).[9,10] As previously observed, rate constants for charge separation are dependent

* Address correspondence to either author. E-mail: lewis@chem.nwu.edu or wasielew@chem.nwu.edu.

(1) (a) Lewis, F. D. In *Electron Transfer in Chemistry*; Balzani, V., Ed.; Wiley-VCH: Weinheim, Germany, 2001; Vol. 3. (b) Holmlin, R. E.; Dandliker, P. J.; Barton, J. K. *Angew. Chem., Int. Ed. Engl.* **1997**, *36*, 2714−2730. (c) Giese, B. *Acc. Chem. Res.* **2000**, *33*, 631−636. (d) Schuster, G. B. *Acc. Chem. Res.* **2000**, *33*, 253−260. (e) Nakatani, K.; Dohno, C.; Saito, I. *J. Am. Chem. Soc.* **2000**, *122*, 5893−5894. (f) Shafirovich, V. Y.; Dourandin, A.; Huang, W.; Luneva, N. P.; Geacintov, N. E. *Phys. Chem. Chem. Phys.* **2000**, *2*, 4399−4408.
(2) (a) Lewis, F. D.; Letsinger, R. L.; Wasielewski, M. R. *Acc. Chem. Res.* **2001**, *34*, 159−170. (b) Lewis, F. D.; Wu, Y. *J. Photochem. Photobiol. C* **2001**, *2*, 1−16.
(3) Lewis, F. D.; Wu, T.; Zhang, Y.; Letsinger, R. L.; Greenfield, S. R.; Wasielewski, M. R. *Science* **1997**, *277*, 673−676.
(4) Lewis, F. D.; Liu, X.; Liu, J.; Miller, S. E.; Hayes, R. T.; Wasielewski, M. R. *Nature* **2000**, *406*, 51−53.
(5) Lewis, F. D.; Kalgutkar, R. S.; Wu, Y.; Liu, X.; Liu, J.; Hayes, R. T.; Wasielewski, M. R. *J. Am. Chem. Soc.* **2000**, *122*, 12346−12351.
(6) Marcus, R. A. *J. Chem. Phys.* **1956**, *24*, 966−978.
(7) Sugiyama, H.; Saito, I. *J. Am. Chem. Soc.* **1996**, *118*, 7063−7068.
(8) Voityuk, A. A.; Jortner, J.; Bixon, M.; Rösch, N. *Chem. Phys. Lett.* **2000**, *324*, 430.
(9) For a preliminary account, see the following.
(10) Lewis, F. D.; Liu, X.; Miller, S. E.; Wasielewski, M. R. *J. Am. Chem. Soc.* **1999**, *121*, 9746−9747.

10.1021/ja027108u CCC: $22.00

Chart 1

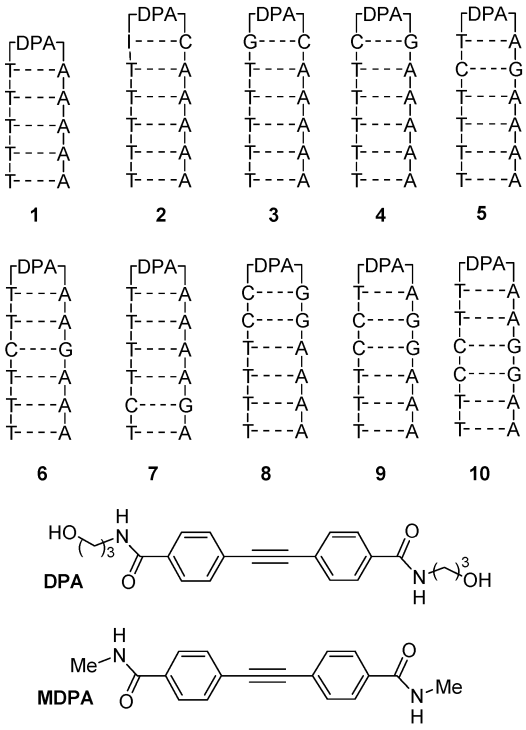

upon the identity of the nucleobase adjacent to the DPA linker that serves as the electron donor (D).[5] However, they are independent of the identities of the other nucleobases in the hairpin stem, in accord with the formation of a localized contact radical ion pair. In contrast, rate constants for charge recombination are dependent upon the identity of the base adjacent to the radical ion pair, indicative of the stabilization of the contact radical ion pair by the adjacent base.

Experimental Section

General Methods. The methods employed for steady-state absorption and fluorescence spectroscopy, the measurement of fluorescence lifetimes, and transient absorption spectroscopy of hairpin-forming bis(oligonucleotide) conjugates have been previously described.[11] Recent modifications have incorporated multichannel data collection with a CCD spectrograph (Ocean Optics, SD2000) for time-resolved spectral information (450−800 nm). The continuum was generated in a sapphire disk using a set of reflective optics and coupled into a 400-μm diameter fiberoptic cable after the sample cell and, thereafter, input into the CCD detector. Typically, 7000 excitation pulses were averaged to obtain the transient spectrum at a particular delay time. The CCD spectrograph, the delay line, and the shutters were driven by a computer-controlled system. In-house LabView (National Instruments) software routines allowed automatic spectral acquisition over a series of delay line settings. Kinetic traces at appropriate wavelengths were assembled from the accumulated spectral data. The instrument response function in the pump−probe experiments was ~150 fs. The sample solutions for transient measurements contained 1×10^{-5} M conjugate in standard buffer (0.1 M NaCl, 30 mM sodium phosphate, pH 7.2) and had an absorbance of 0.1−0.2 at the excitation wavelength in a 2-mm path length cuvette. The absorption spectra of the solutions were measured before and after the experiment to check for possible sample decomposition. The samples were stirred during the experiment using a wire stirrer to prevent thermal lensing and sample degradation.

(11) Lewis, F. D.; Wu, T.; Liu, X.; Letsinger, R. L.; Greenfield, S. R.; Miller, S. E.; Wasielewski, M. R. *J. Am. Chem. Soc.* **2000**, *122*, 2889−2902.

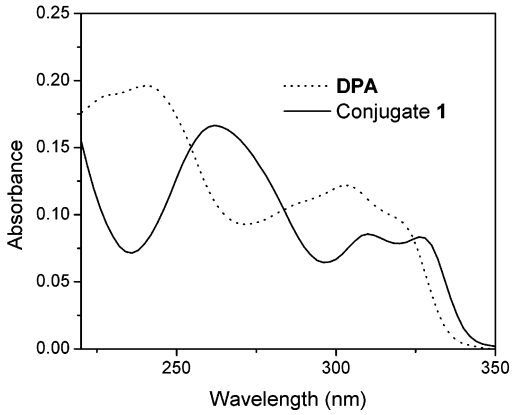

Figure 1. Electronic absorption spectra of diol DPA in aqueous solution and conjugate **1** (2×10^{-6} M) in standard buffer (0.1 M NaCl, 30 mM sodium phosphate, pH 7.2).

Materials. Diphenylacetylene-4,4′-dicarboxylic acid was prepared from stilbene-4,4′-dicarboxylic acid via bromination−dehydrobromination and converted to the dimethylamide MDPA (Chart 1), as previously described,[12] and to the diol DPA, as described for the analogous stilbene diol by Letsinger and Wu.[13] The reaction of excess diol DPA with 4,4′-dimethoxytrityl chloride yielded the mono-DMT protected diol, which was reacted with 2-cyanoethyl diisopropylchlorophosphoramidite to yield the monoprotected, monoactivated diol. The bis(oligonucleotide) conjugates **1**−**10** (Chart 1) were prepared by means of conventional phosphoramidite chemistry using a Millipore Expedite oligonucleotide synthesizer, following the procedure developed by Letsinger and Wu for related bis(oligonucleotide) conjugates.[13] The conjugates were first isolated as trityl-on derivatives by RP HPLC, detritylated in 80% acetic acid for 30 min, and then repurified by RP HPLC. A single peak was detected by both RP and IE HPLC. Molecular weights were determined by means of electrospray ionization mass spectroscopy with a Micromass Quattro II Atmospheric Pressure Ionization (API) Spectrometer.

Results and Discussion

Spectra and Structure. The absorption spectra of DPA and conjugate **1** are shown in Figure 1. The UV absorption spectra of the conjugates **1**−**10** display maxima at wavelengths longer than 300 nm, assigned to the DPA chromophore, and near 260 nm, assigned to the overlapping absorption of the nucleobases and DPA (Figure 1). The two maxima in the long wavelength band of **1** are red-shifted and altered in relative intensity compared with the absorption spectrum of DPA. The red-shift is similar to that observed by Nastasi et al.[14] for quinacrine−DNA complexes and is attributed to weak ground-state interactions between the intercalated chromophore and neighboring base pairs.

The absorption spectra of **1** at several temperatures are shown in Figure 2. At high temperature, the long wavelength band of **1** resembles that of DPA. The temperature dependence of the 260- and 327-nm absorption intensities for **1** are shown in Figure 3. Similar thermal profiles were obtained for **4**. The derivatives of these curves provide melting temperatures (T_m) of 55 and 70 °C for **1** and **4**, respectively. These T_m values are ~30 °C higher than those calculated for hypothetical duplex structures

(12) Lewis, F. D.; Yang, J. S.; Stern, C. S. *J. Am. Chem. Soc.* **1996**, *118*, 12029−12037.
(13) Letsinger, R. L.; Wu, T. *J. Am. Chem. Soc.* **1995**, *117*, 7323−7328.
(14) Nastasi, M.; Morris, J. M.; Rayner, D. M.; Seligy, V. L.; Szabo, A. G.; Williams, D. F.; Yip, R. W. *J. Am. Chem. Soc.* **1976**, *98*, 3979−3986.

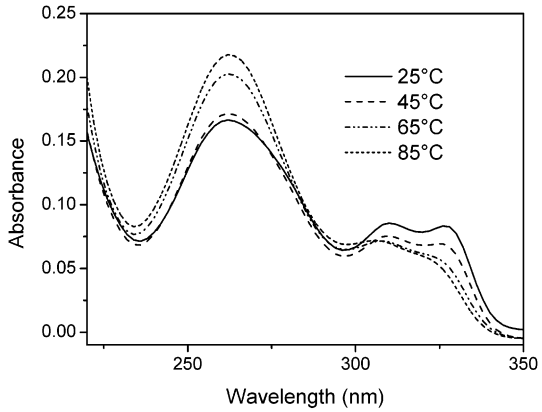

Figure 2. Temperature dependence of the electronic absorption spectra of conjugate **1** in standard buffer.

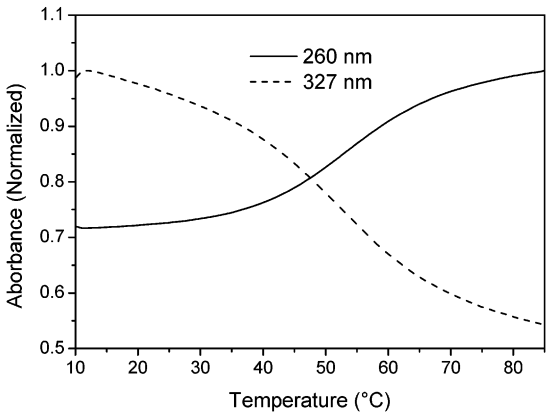

Figure 3. Thermal dissociation profile for conjugate **1** in standard buffer monitored at 260 and 327 nm.

formed between two self-complementary conjugates.[15] Increasing the concentration of **1** from 0.35 OD to 0.94 OD at 327 nm does not change its T_m, in accord with the formation of hairpin rather than duplex structures. This indicates that hairpin melting can be described using a simple two-state model in which π-stacking between the base pairs and between the DPA chromophore and the adjacent A/T base pair is disrupted simultaneously.[16] The T_m value for **4** is similar to that for a stilbenedicarboxamide-linked hairpin with a stem consisting of six T/A base pairs.[13] Values of T_m were not determined for the other conjugates but are assumed to be >50 °C, on the basis of their structures.

The DPA-linked conjugates are believed to adopt hairpin structures similar to that of a stilbenediether-linked conjugate for which the crystal structure has been determined and shown to possess classic B-DNA geometry.[17] The circular dichroism spectrum of **1** is shown in Figure 4 along with that of poly(dA)/poly(dT), which is known to form a B-DNA duplex.[16] The CD spectrum of **1** is broader, as expected for a duplex with only five base pairs; however, it displays a positive band at 283 nm and a negative band at 248 nm, characteristic of B-DNA.[16] No CD band is observed at wavelengths longer than 300 nm, as previously observed for stilbenedicarboxamide-linked hairpins.[11] The CD spectrum of **4** is similar to that of **1**. The minimized structure of **1** obtained from MM2 calculations is shown in Figure 5. The DPA chromophore is approximately parallel to the adjacent A/T base pair, and the calculated average DPA−T/A plane-to-plane distance is 3.8 Å, somewhat larger than the 3.4-Å average π-stacking distance in B-DNA. However, the effect of melting on the long-wavelength absorption band of **1** (Figures 2 and 3) indicates that there is a weak electronic interaction between the DPA chromophore and the adjacent base pairs in these hairpin structures.

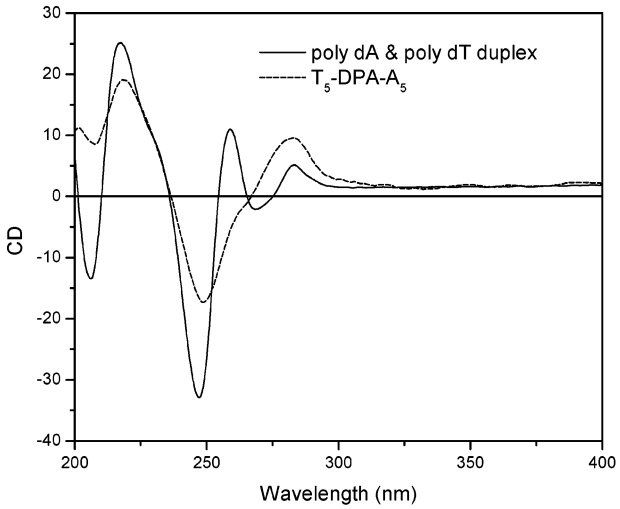

Figure 4. Circular dichroism spectra of poly(dA)/poly(dT) and conjugate **1** in standard buffer.

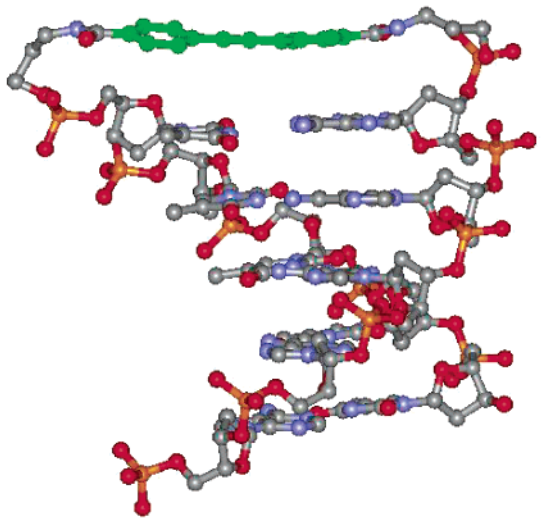

Figure 5. MM2-minimized structure for conjugate **1**. The DPA linker is at the top of the structure.

DPA is strongly fluorescent in methanol solution, having a fluorescence maximum at 351 nm and a fluorescence quantum yield of 0.33. The fluorescence decay time is similar to the 0.5-ns instrument response function of our lifetime apparatus. Diphenylacetylene and some of its derivatives display dual S_2 and S_1 fluorescence as a consequence of slow internal conversion.[18] However, 4-carbomethoxydiphenylacetylene displays only S_1 florescence. The absorption and fluorescence of diol DPA also display a mirror image relationship, as expected for S_1 fluorescence.

(15) Breslauer, K. J.; Frank, R.; Blöcker, H.; Marky, L. A. *Proc. Natl. Acad. Sci. U.S.A.* **1986**, *83*, 3746−3750.
(16) Bloomfield, V. A.; Crothers, D. M.; Tinoco, I., Jr. *Nucleic Acids, Structures, Properties, Functions*; University Science Books: Sausalito, CA, 2000.
(17) Lewis, F. D.; Liu, X.; Wu, Y.; Miller, S. E.; Wasielewski, M. R.; Letsinger, R. L.; Sanishvili, R.; Joachimiak, A.; Tereshko, V.; Egli, M. *J. Am. Chem. Soc.* **1999**, *121*, 9905−9906.
(18) Hirata, Y. *Bull. Chem. Soc. Jpn.* **1999**, *72*, 1647−1664.

Chart 2

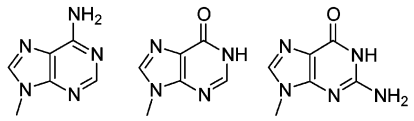

Freshly prepared solutions of conjugates **1**, **5**−**7**, and **9**−**10**, which possess a T/A base pair adjacent to the DPA linker, are weakly fluorescent ($\Phi_f < 10^{-3}$) with spectra similar in appearance to that of DPA. Stronger fluorescence with an emission maximum of 390 nm can readily be detected after a single scan of the fluorescence spectrum and increases in intensity with repeated scans. This emission is attributed to a fluorescent photoproduct; however, no attempts were made to identify this product. The conjugates **3**, **4**, and **8**, which possess a G/C base pair adjacent to the DPA linker, are nonfluorescent and do not display product fluorescence upon exposure to light. Efficient quenching of DPA fluorescence in all of the conjugates is attributed to an electron-transfer process in which the DPA chromophore serves as an electron acceptor and a nucleobase as the electron donor. The driving force for photoinduced charge separation can be calculated using Weller's equation (eq 1)

$$\Delta G_{cs} = E_{ox} - E_{red} - E_S + C \qquad (1)$$

where E_S is the DPA singlet energy (3.76 eV), E_{red} is the DPA reduction potential (−1.98 V vs SCE in DMSO) solution, E_{ox} is the nucleobase oxidation potential (Chart 2),[19] and C is a constant determined by the solvent-dependent Coulombic attraction energy and the Born solvation energy of the ions.[20] If the value of C is small, then charge separation should be exergonic for all of the electron donor nucleobases.

Transient Absorption Spectra. The transient absorption spectra of diol DPA and the conjugates **1**−**10** were measured with a femtosecond amplified titanium−sapphire based laser system that has been described previously.[11] An ∼110-fs, 330-nm laser pulse is used to excite the samples, and a white light probe pulse of the same duration is used to monitor the spectra as a function of time.

The transient absorption spectrum of diol DPA in methanol solution consists of a strong band with a maximum at 535 nm. Spectra recorded at 5, 50, and 250 ps after the exciting pulse have identical band shapes. The decay of the transient monitored at 535 nm is best fit by a biexponential function with decay times of 12 and 206 ps (relative amplitudes, 15 and 85%, respectively). The transient absorption spectrum of DPA in methanol is similar in appearance to that of 4-carbomethoxydiphenylacetylene (λ_{max} = 500 nm).[18] The DPA transient absorption maximum is at a longer wavelength, and the decay time of its principal decay component is faster (206 ps vs 700 ps) than that of 4-carbomethoxydiphenylacetylene. The minor 12-ps decay component may reflect a solvent or DPA structural relaxation processes.

The absorption spectrum of the anion radical of the MDPA (Chart 1) was obtained by spectroelectrochemistry in tetrahydrofuran solution at a potential of −2.4 V vs SCE. The spectrum consists of a band with a maximum at 564 nm and a shoulder at 503 nm. The spectrum is similar in band shape to that reported by Suzuki et al.[21] for the diphenylacetylene anion radical (λ_{max} = 446 nm).

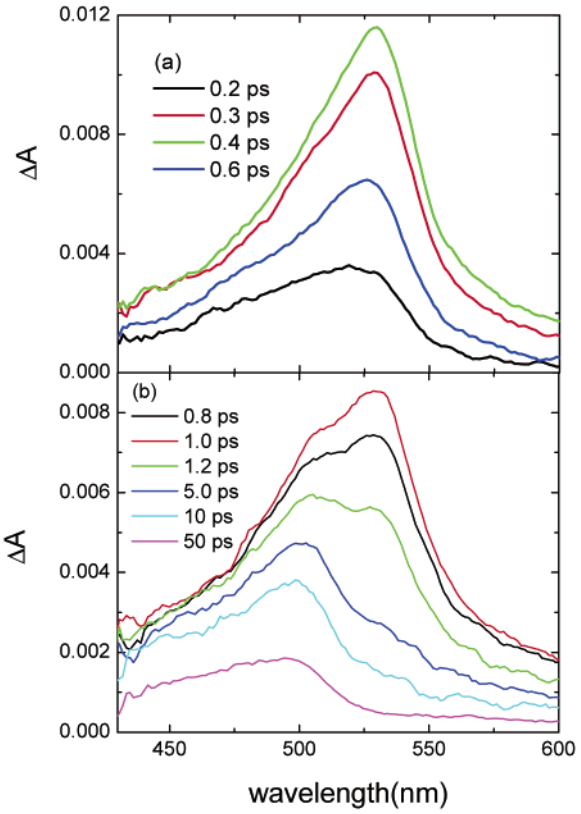

Figure 6. Transient absorption spectra of conjugate **5** obtained after a 0.11-ps 330-nm excitation pulse at indicated delay times: (a) formation of the 535-nm transient (^{1}DPA*) and (b) formation and decay of the 500-nm transient (DPA$^{\bullet-}$).

The transient absorption spectra of conjugate **5** in aqueous solution (0.1 M NaCl in 10 mM sodium phosphate, pH 7.2 buffer) at delay times of 0.2−50 ps are shown in Figure 6. During the first 0.6 ps following excitation, a transient with a 535-nm absorption maximum and a band shape similar to that of DPA grows in intensity (Figure 6a). Monitoring the 535-nm kinetics provides a rise time of 0.2 ps, similar to the 0.15-ps instrument response function. During the time period 0.8−50 ps following excitation, the 535-nm band decays and the absorption maximum shifts to 500 nm (Figure 6b). Similar time-dependent transient absorption spectra are seen for all of the DPA-linked conjugates **1**−**10**.[22] The transient absorption spectrum of **5** observed at delay times > 5 ps (Figure 6b) has a band shape similar to that of MDPA$^{\bullet-}$. On the basis of these band shape comparisons, the 535- and 500-nm transients are assigned to ^{1}DPA* and DPA$^{\bullet-}$, respectively. The blue-shift for DPA$^{\bullet-}$ versus ^{1}DPA* (500 nm vs 535 nm) is similar to that observed for the parent, unsubstituted diphenylacetylene (446 nm for the anion radical in tetrahydrofuran[21] vs 500 nm for the singlet state in hexane solution[18]). The difference in these transient absorption maxima is much larger than that observed

(19) Oxidation potentials are for the nucleosides in acetonitrile solution versus SCE. Values are from: Seidel, C. A. M.; Schulz, A.; Sauer, M. H. M. *J. Phys. Chem.* **1996**, *100*, 5541−5553.
(20) Weller, A. *Zeit. Phys. Chem. Neue. Folg.* **1982**, *133*, 93−98.
(21) Suzuki, H.; Koyano, K.; Shida, T.; Kira, A. *Bull. Chem. Soc. Jpn.* **1982**, *55*, 3690−3701.
(22) The transient absorption spectra for hairpin **1** have previously been published.

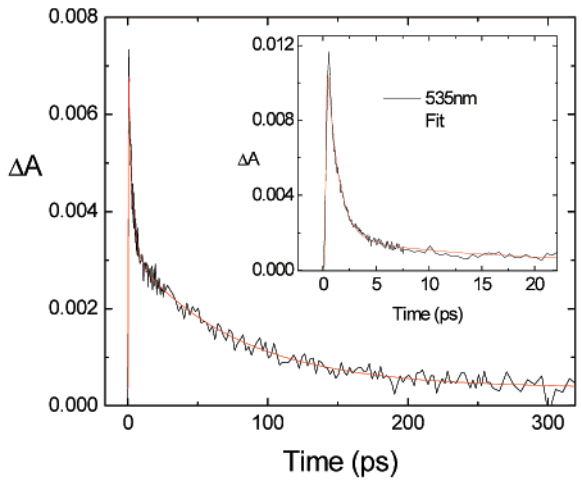

Figure 7. Transient absorption kinetics for conjugate **5** monitored at 500 nm following a 0.11-fs, 330-nm excitation. Inset shows kinetics monitored at 535 nm.

Table 1. Singlet and Anion Radical Decay Times and Rate Constants for Charge Separation and Charge Recombination for the DPA-linked Conjugates

conjugate	τ_s,[a] ps	τ_a,[b] ps	10^{-12} k_{cs},[c] s^{-1}	10^{-9} k_{cr},[d] s^{-1}
1	2.7	1400	0.37	0.71
2	1.9	102	0.53	9.8
3	0.5	19	2.0	52
4	0.4	21	2.5	48
5	2.3	77	0.43	13
6	2.7	1400	0.37	0.71
7	1.8	1500	0.56	0.67
8	0.2	11	5.0	91
9	2.4	85	0.42	12
10	3.0	3000	0.33	0.33

[a] Decay of the 535-nm transient in nitrogen-purged standard buffer solution. Estimated error ± 10% of the reported value; minimum error ± 0.1 ps. [b] Decay of the 500-nm transient. Estimated error ± 10% of the reported value. [c] $k_{cs} = \tau_s^{-1}$. [d] $k_{cr} = \tau_a^{-1}$.

for the stilbene-dicarboxamide anion radical versus singlet (<5 nm),[11] facilitating the assignment of transient spectra and decay components of the DPA-linked hairpins.

The decays of the transient absorption spectra of **5** monitored at the absorption maxima of ^{1}DPA* (535 nm) and DPA$^{\bullet-}$ (500 nm) are shown in Figure 7 and are best fit by biexponential functions. The relative amplitude of the shorter-lived (^{1}DPA*) component is larger at 535 nm, and that of the longer lived component (DPA$^{\bullet-}$) is larger at 500 nm. Decay times for the singlet and anion radical obtained from the 535 and 500 nm decays, respectively, for conjugates **1**−**10** are reported in Table 1. In some cases, a rising component could be resolved at 500 nm, with a rise time similar to that of the fast decay of the 535-nm transient. Neither the absorption spectra of the conjugates nor the observed decay times change during the course of data collection, indicating that the fluorescent product observed from some of the conjugates does not interfere with the transient absorption experiments.

A kinetic scheme for photoinduced charge separation and charge recombination is shown in Figure 8, along with the thermodynamics for these relationships. The free energy for charge separation and charge recombination can be estimated from Weller's equation (eq 1) and from the sum of the redox potentials ($\Delta G_{cr} = E_{red} - E_{ox}$), respectively. Since the singlet decay times are much shorter than that of the diol DPA, the

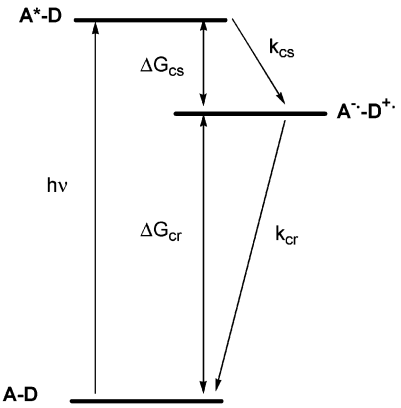

Figure 8. Kinetic scheme and thermodynamics of charge separation and charge recombination. A is the acceptor linker chromophore, and D is the nucleobase donor.

singlet decay times are determined by the rate constant for charge separation ($\tau_s^{-1} = k_{cs}$). Similarly, the anion radical decay times are determined by the rate constant for charge recombination ($\tau_a^{-1} = k_{cr}$). Values of k_{cs} and k_{cr} are reported in Table 1.

Charge Separation Dynamics. Hairpins **1**−**4** have nearest-neighbor T/A, I/C, G/C, and C/G base pairs, respectively, located between the DPA linker and a poly(T/A) hairpin stem. We previously reported that values of k_{cs} increase in the series **1** < **2** < **3**, as ΔG_{cs} becomes more exergonic (−0.09, −0.38, and −0.54 V for photooxidation of A, I, and G, respectively).[5] On a Marcus plot of log(k_{cs}) versus $-\Delta G$, these data points lie near the top of the Marcus curve, thus accounting for the small variation in k_{cs} values. The value of k_{cs} for hairpin **3**, which has a DPA−GT sequence, is similar to that for hairpin **4**, which has a DPA−GA sequence. The value of k_{cs} for **8**, which has a DPA−GG sequence, is larger than that for **4**; however, the difference in τ_s values for **4** and **8** is at the limit of our estimated experimental error (Table 1). Reid et al.[23] have recently reported that the rates of quenching of intercalated thionine dyes by neighboring guanine are similar for GA and GT sequences and slightly faster for GG sequences. Thus, the identity of the neighboring base has, at best, a modest effect on the value of k_{cs} for the oxidation of guanine by ^{1}DPA*.

Hairpins **5**−**7** possess a T/A base pair adjacent to the DPA linker and a single C/G base pair at the second, third, and fifth positions away from the linker, and hairpins **9** and **10** possess a T/A base pair adjacent to the DPA linker and two C/G base pairs at the second and third or third and fourth positions removed from the linker. The values of k_{cs} for all these hairpins are within the experimental error of the value for hairpin **1**, except for hairpin **8**, which inexplicably has a somewhat larger value of k_{cs}.

The similar values of k_{cs} for **1**, **5**−**7**, and **9**−**10** indicates that hole injection to a guanine separated from DPA by one or more base pairs does not compete with the contact radical ion pair formation in the present system. Both we[11] and Michel-Beyerle[24] have reported studies of hole injection into DNA in which no charge separation occurs between weaker acceptors (stilbene-dicarboxamide and an acridinium ion) and an adjacent T/A base pair, but bridge-mediated hole injection does occur to a guanine

(23) Reid, G. D.; Whittaker, D. J.; Day, M. A.; Turton, D. A.; Kayser, V.; Kelly, J. M.; Beddard, G. S. *J. Am. Chem. Soc.* **2002**, *124*, 5518−5527.
(24) Hess, S.; Götz, M.; Davis, W. B.; Michel-Beyerle, M. E. *J. Am. Chem. Soc.* **2001**, *123*, 10046−10055.

or deazaguanine base when one or more T/A base pairs are located between the excited acceptor and nucleobase donor. Zewail and co-workers[25] report relatively slow quenching of singlet aminopurine (Ap) by neighboring A and enhanced quenching for the sequence Ap−AG versus Ap−AI (τ_s = 65 vs 260 ps). Enhanced quenching was attributed to the simultaneous nearest-neighbor quenching by A and bridge-mediated quenching by G. The calculated value of $k_{cs} = 4 \times 10^9$ for quenching by A in the sequence Ap−AI is much slower than the value of $k_{cs} = 3.7 \times 10^{11}$ observed for conjugate **1**. The relatively low value of k_{cs} for nearest-neighbor quenching in the system Ap−AG might facilitate detection of bridge-mediated superexchange quenching by G. Alternatively, charge separation in the Ap−AG system may occur via a thermally induced, bridge-mediated hopping mechanism rather than tunneling,[26] thus complicating kinetic analysis.

The absence of a significant modulation of the values of k_{cs} by the adjacent base in the DPA-linked hairpins is, at first, surprising. According to the semiempirical calculations of Voityuk et al.[8] for nucleobase cation radical triads, the relative energies of $YG^{\bullet+}X$ with different neighboring bases increases in the order $YG^{\bullet+}G < YG^{\bullet+}A < YG^{\bullet+}T$ by a significant amount (relative energies = 0, 0.13, and 0.26 eV, respectively). Similarly, the calculated energy difference between a $YA^{\bullet+}A$ and $YA^{\bullet+}G$ sequence is 0.13 eV. An effect of this magnitude could easily account for the decrease in singlet lifetime observed by Zewail for the sequence Ap−AG versus Ap−AI.[25] Several possible explanations for the apparent disagreement between our experimental results and theory can be considered. First, since the values of k_{cs} for **1** and **3** are very fast and near the top of the Marcus curve, a further increase in the exothermicity of electron transfer (eq 1) might not result in a measurable increase in k_{cs}. Alternatively, ultrafast geminate charge separation may result in the formation of a contact radical ion pair in which the positive charge is initially localized on a single nucleobase. Since the difference in k_{cs} values for nearest-neighbor quenching by G versus A in hairpins **1** and **3** or **4** can readily be distinguished, we favor the later explanation, formation of a localized contact radical ion pair with little or no participation of the base adjacent to the radical ion pair. This conclusion is in agreement with that of Reid et al.,[23] which is based on a less direct analysis of quenching of intercalated thionine by guanine but not adenine.

Charge Recombination Dynamics. Values of k_{cr} decrease for the series **3** > **2** > **1** as ΔG_{cr} becomes more exergonic (−3.20, −3.45, and −3.67 eV for G, I, and A, respectively). On a plot of log(k_{cr}) versus ΔG_{cr}, these data points lie deep in the Marcus inverted region and display the expected quasi-linear dependence upon ΔG_{cr}.[5] Values of k_{cr} for hairpins **3** and **4** are similar, suggestive of similar ion pair energies for the sequences DPA−GT and DPA−GA. However, the value of k_{cr} for conjugate **8**, which has a DPA−GG sequence, is twice as large as that of **4**, which has a DPA−GA sequence. An even larger increase in the value of k_{cr} is observed for conjugate **5** versus **1**, which have DPA−AG and DPA−AA sequences, respectively.

The significantly larger value of k_{cr} for **5** versus **1** is indicative of a change in the nature of the contact radical ion pair prior to charge recombination. The relaxation process could result in (a) charge migration from A to G, (b) charge delocalization between A and G, or (c) stabilization of the contact radical ion pair by interaction with the neighboring G. Charge migration would lead to a larger donor−acceptor distance, most likely resulting in a smaller value of k_{cr} rather than the larger value that is observed (Table 1). Charge migration from $A^{\bullet+}$ to G clearly does not occur over longer distances, since the values of k_{cr} for conjugates **1**, **6**, and **7** are similar, as are the values for **1** and **10**.

Charge delocalization in DNA is currently a topic of debate among theoreticians, some favoring extensive delocalization[27] and others localization on a single nucleobase.[28] The effect of charge delocalization over the AG doublet in the DPA−AG sequence of conjugate **5** on the value of k_{cr} is difficult to predict. However, charge delocalization in conjugate **9**, which has a DPA−AGG sequence, should be even more favorable than charge delocalization in **5**, which has a DPA−AGA sequence. The similar values of k_{cr} for conjugates **5** and **9** suggest that the cation radicals are not delocalized in these systems.

We are left with explanation c, stabilization of the initially formed $DPA^{\bullet-}-A^{\bullet+}G$ contact radical ion pair by interaction with an adjacent guanine. This would result in a lower ion pair energy and a more rapid charge recombination (Marcus inverted region behavior). The observation of values of k_{cr} for hairpins **5** and **9** similar to that for **2**, which possesses an I/C base pair adjacent to DPA, suggests that the AG stabilization energy might be similar to the difference in oxidation potentials for A versus I. The difference in single nucleotide oxidation potentials is ∼0.3 V (Chart 2). However, base stacking is believed to have a leveling effect on the differences in oxidation potentials in the duplex environment.[26] Thus, the actual ion pair stabilization may be closer to the value of 0.13, calculated by Voityuk et al.[29] for base triads containing $A^{\bullet+}A$ versus $A^{\bullet+}G$ sequences. A similar, but smaller, ion pair stabilization energy can account for the faster charge recombination of **8** versus **5**.

Hole Migration Energetics. The failure to observe hole migration to yielding a radical ion pair separated by intervening neutral base pairs indicates that the $DPA^{\bullet-}-A^{\bullet+}G$ contact radical ion pair is more stable than the $DPA^{\bullet-}-AG^{\bullet+}$ base-separated ion pair, even though the hole resides on adenine in the contact ion pair and on guanine in the base-pair-separated ion pair. The free energy change for this charge migration process (ΔG_{cm}) depends primarily upon the difference in Coulomb attraction energies of the two ion pairs, which can be described by eq 2

$$\Delta G_{cm} = \frac{e_o^2}{\epsilon}\left(\frac{1}{r_{DA1}} - \frac{1}{r_{DA2}}\right) \qquad (2)$$

where e_o is the atomic unit of charge, ϵ is the solvent dielectric constant, and r_{DA1} and r_{DA2} are the distances between the contact and base-separated radical ion pairs, respectively. The values of r_{DA1} and r_{DA2} are estimated to be 3.4 and 6.8 Å, on the basis

(25) Wan, C.; Fiebig, T.; Schiemann, O.; Barton, J. K.; Zewail, A. H. *Proc. Natl. Acad. Sci. U.S.A.* **2000**, *97*, 14052−14055.
(26) Bixon, M.; Jortner, J. *J. Am. Chem. Soc.* **2001**, *123*, 12556−12567.
(27) (a) Conwell, E. M.; Basko, D. M. *J. Am. Chem. Soc.* **2001**, *123*, 11441−11445. (b) Barnett, R. N.; Cleveland, C. L.; Joy, A.; Landman, U.; Schuster, G. B. *Science* **2001**, *294*, 567−574.
(28) (a) Olofsson, J.; Larsson, S. *J. Phys. Chem. B* **2001**, *105*, 10398−10406. (b) Kurnikov, I. V.; Tong, G. S. M.; Madrid, M.; Beratan, D. N. *J. Phys. Chem. B* **2002**, *106*, 7−10.
(29) Voityuk, A. A.; Michel-Beyerle, M. E.; Rösch, N. *Chem. Phys. Lett.* **2001**, *342*, 231−238.

of the average π-stacking distance in B-DNA. An upper bound for the value of $\Delta G_{cm} \approx 0.4$ eV can be estimated from the difference between the oxidation potentials of G and A (Chart 2) or the difference in their adiabatic ionization potentials.[30] A smaller value of $\Delta G_{cm} \approx 0.2$ eV was estimated by Bixon and Jortner[26] on the basis of their analysis of kinetic data for charge migration. Using an average value of 0.3 eV, eq 2 predicts that the minimum effective dielectric constant necessary to support charge migration is ~7. This value is similar to that estimated by Weller[20] and by Masuhara and Mataga[31] for the conversion of contact to solvent separated radical ion pairs in solution.

The effective polarity in the hydrophobic π-stacked core of DNA has been the subject of conjecture.[10] Mazur and Jernigan[32] assume a low value ($\epsilon \approx 2-4$) in their analysis of the electrostatic contributions to DNA base-stacking interactions. Tavernier and Fayer[33] suggest that the dielectric constant of pyridine ($\epsilon = 12.4$) provides a more realistic approximation. Williams and Barton[34] recently reported an estimated value of $\epsilon \approx 100$ using a one-dimensional point charge model. Since our analysis is based on the behavior of the $DPA^{\bullet-}-A^{\bullet+}$ contact radical ion pair that is located at the end of the hairpin, its relevance to the π-stacked core of DNA remains to be established.

Concluding Remarks. Femtosecond pulsed laser excitation of the DPA-linked hairpins **1**−**10** results in the population of ^{1}DPA* followed by charge separation with decay times ranging from 0.2 to 3.0 ps to form $DPA^{\bullet-}$. The dynamics of charge separation depend weakly on the oxidation potentials of the neighboring nucleobase (A, I, or G), as expected for an ultrafast exergonic electron-transfer process which occurs near the top of the Marcus curve.[5] Values of k_{cs} are also weakly dependent upon the identity of nonnearest-neighbor base. This indicates that the charge separation process yields a contact radical ion pair in which the positive charge is initially localized on the neighboring nucleobase. There is no evidence for a single-step charge injection to more remote bases in these hairpin systems. It is important to emphasize that charge injection to remote bases does occur in systems where the electron acceptor can oxidize the remote base but not the adjacent base.[3,24,25]

The contact radical ion pairs formed by charge separation decay via charge recombination with decay times ranging from 11 ps to 3 ns. The values of k_{cs} are dependent upon the oxidation potential of the neighboring nucleobase, as expected for highly exergonic electron transfer in the Marcus inverted region.[5] The rate constants for charge recombination are also dependent upon the identity of the nucleobase adjacent to the contact radical ion pair but not upon the identity of more remote nucleobases. This dependence is attributed to stabilization of the contact radical ion pair via interaction with its nearest-neighbor base, analogous to the conversion of a charge-transfer stabilized $A^{\bullet-}D^{\bullet+}$ exciplex to a $A^{\bullet-}D^{\bullet+}D$ triplex.[35] Again, it is important to emphasize that charge migration does take place for base-separated radical ion pairs formed via bridge-mediated electron transfer in DNA.[3,4,24,25,36]

The absence of hole migration in the initially formed contact radical ion pair to yield a base-separated ion pair is attributed to the distance dependence of the Coulomb attraction energy (eq 2). The failure to observe hole migration from adenine to guanine suggests that the effective dielectric constant for the $DPA^{\bullet-}-A^{\bullet+}$ contact radical ion pair is < 7. An important practical consequence of charge localization in the singlet contact radical ion pair is that charge recombination is both rapid and efficient. This effectively precludes the use of strong singlet acceptors in studies of charge migration in DNA.[37] In our investigations of charge migration, we have found it necessary to initially inject a charge to a guanine primary donor separated from the acceptor by three or four base pairs, thus largely overcoming the Coulombic attraction between the donor and acceptor radical ions.[4,36,38]

Acknowledgment. This research is supported by grants from the Division of Chemical Sciences, Office of Basic Energy Sciences, U.S. Department of Energy under contracts DE-FG02-96ER14604 (F.D.L.) and by DE-FG02-99ER14999 (M.R.W.). We thank Peter Dinolfo for the spectroelectrochemical measurements.

JA027108U

(30) Orlov, V. M.; Smirnov, A. N.; Varshavsky, Y. M. *Tetrahedron Lett.* **1976**, *48*, 4377−4378.
(31) Masuhara, H.; Mataga, N. *Acc. Chem. Res.* **1981**, *14*, 312−318.
(32) Mazur, J.; Jernigan, R. L. *Biopolymers* **1991**, *31*, 1615−1629.
(33) Tavernier, H. L.; Fayer, M. D. *J. Phys. Chem. B* **2000**, *104*, 11541−11550.
(34) Williams, T. T.; Barton, J. K. *J. Am. Chem. Soc.* **2002**, *124*, 1840−1841.
(35) Caldwell, R. A.; Creed, D.; DeMarco, D. C.; Melton, L. A.; Ohta, H.; Wine, P. H. *J. Am. Chem. Soc.* **1980**, *102*, 2369−2377.
(36) (a) Lewis, F. D.; Liu, J.; Liu, X.; Zuo, X.; Hayes, R. T.; Wasielewski, M. R. *Angew. Chem., Int. Ed.* **2002**, *41*, 1026−1028. (b) Lewis, F. D.; Liu, X.; Liu, J.; Hayes, R. T.; Wasielewski, M. R. *J. Am. Chem. Soc.* **2000**, *122*, 12037−12038.
(37) Rogers, J. E.; Weiss, S. J.; Kelly, L. A. *J. Am. Chem. Soc.* **2000**, *122*, 427−436.
(38) Lewis, F. D.; Zuo, X.; Liu, J.; Hayes, R. T.; Wasielewski, M. R. *J. Am. Chem. Soc.* **2002**, *124*, 4568−4569.